Electronic Supplementary Material (ESI) for CrystEngComm.

Supporting Information for

Positional isomerism of unsymmetrical semirigid ligands toward the construction of discrete and infinite coordination architectures of zinc(II) and cadmium(II) complexes

Jing-Yun Wu,* Pin-Ting Yuan and Cheng-Chu Hsiao

Department of Applied Chemistry, National Chi Nan University, Nantou 545, Taiwan. Fax: +886-49-2917956. E-mail: jyunwu@ncnu.edu.tw

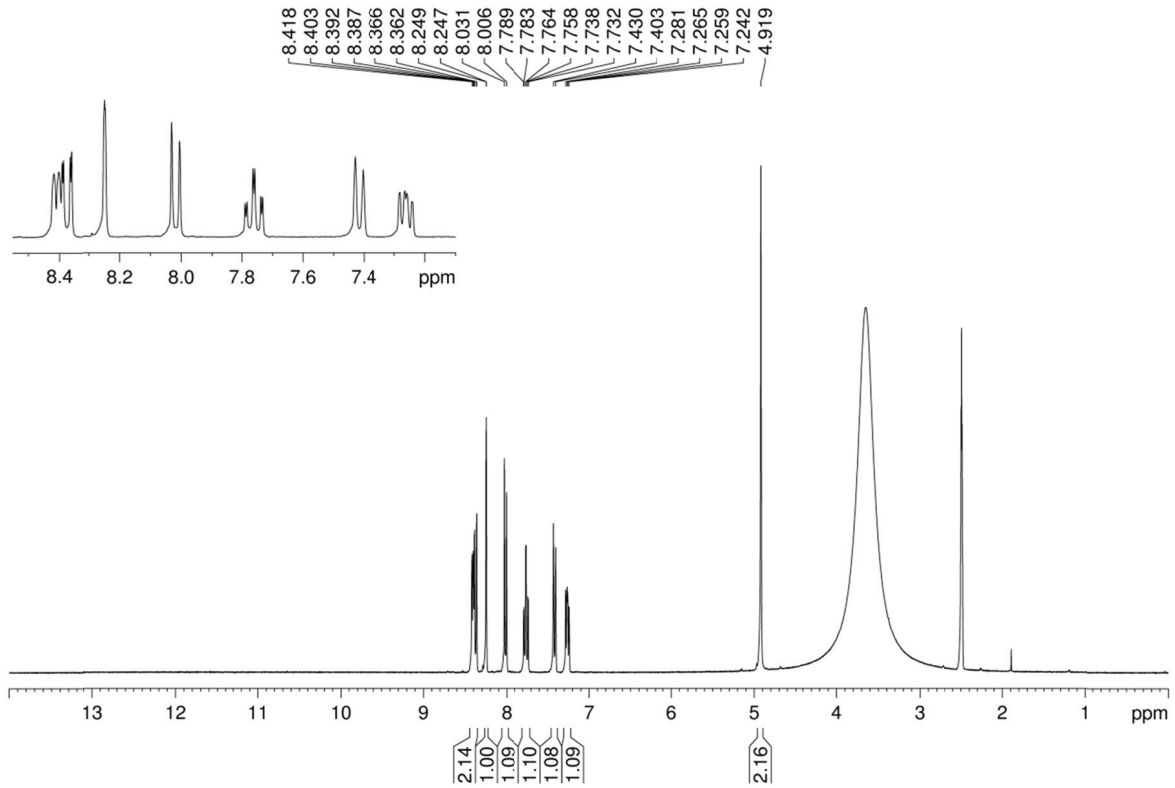

Fig. S1 ^{1}H NMR spectrum of 2-(2-pyridylmethyl)-1,3-dioxoisoindoline-5-carboxylic acid (HInMe-2-py) in DMSO-d_6 at room temperature.

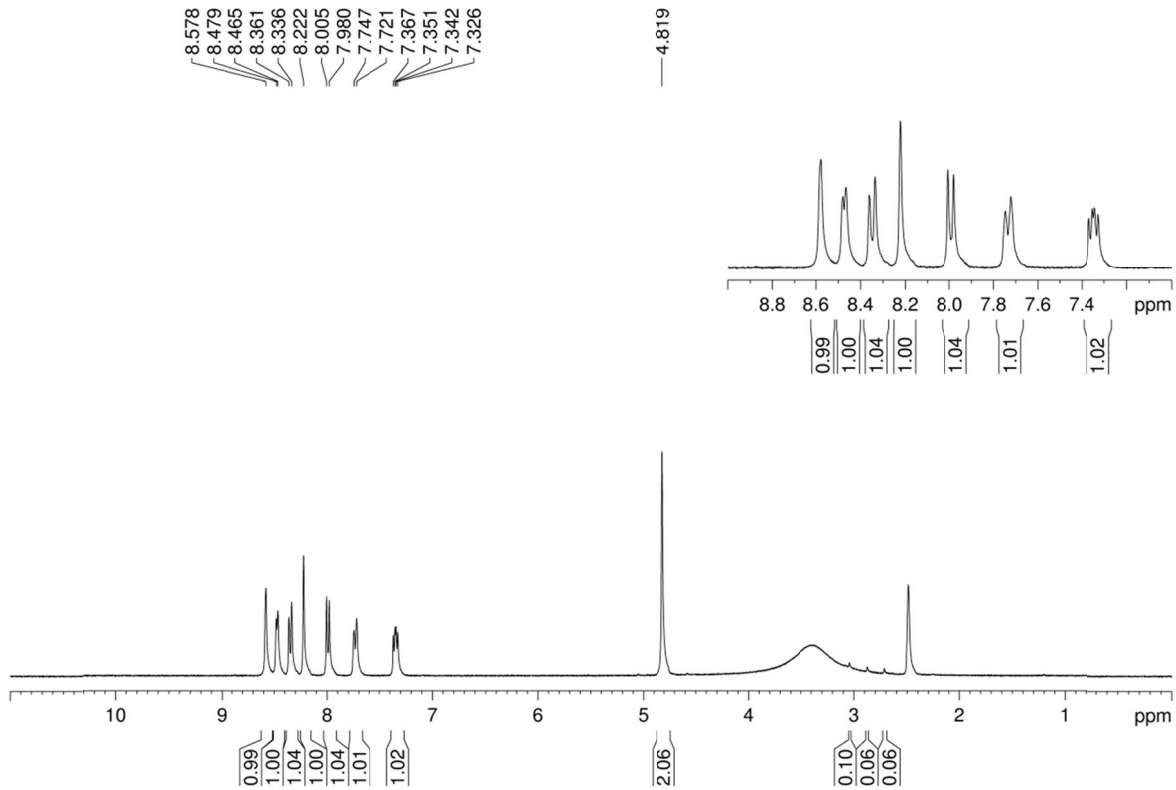

Fig. S2 ^{1}H NMR spectrum of 2-(3-pyridylmethyl)-1,3-dioxoisoindoline-5-carboxylic acid (HInMe-3-py) in DMSO-d_6 at room temperature.

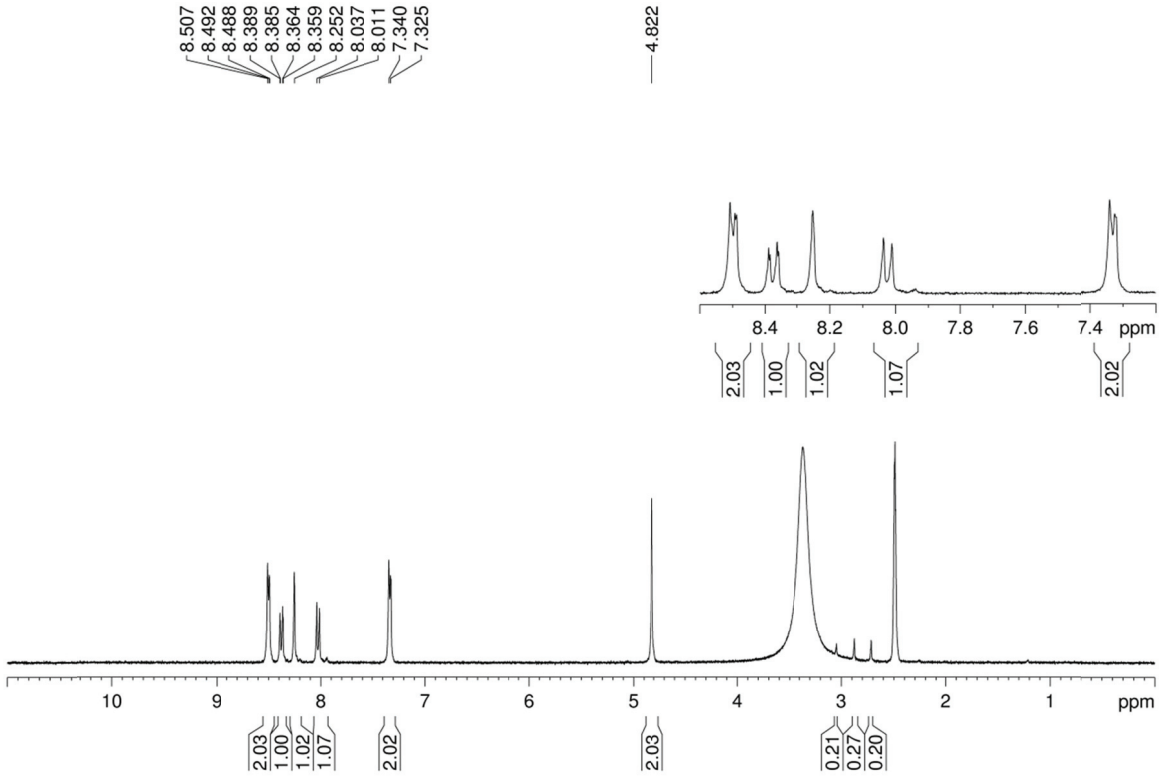

Fig. S3 ^{1}H NMR spectrum of 2-(4-pyridylmethyl)-1,3-dioxoisoindoline-5-carboxylic acid (HInMe-4-py) in DMSO-d_6 at room temperature.

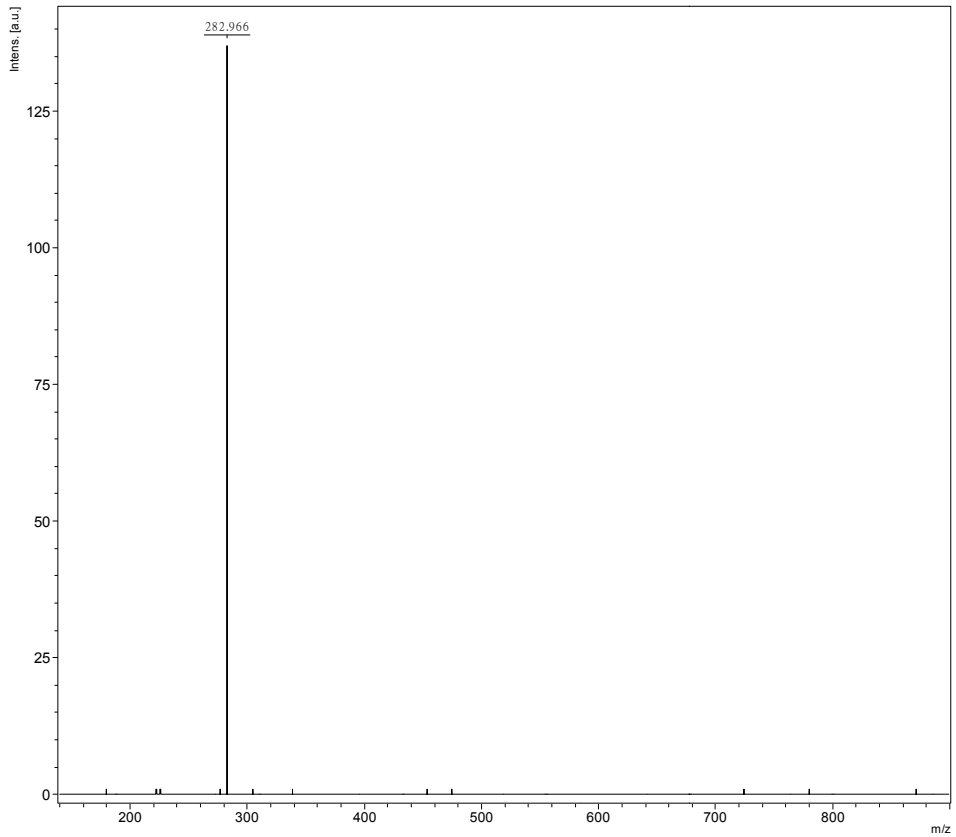

Fig. S4 Matrix-assisted laser desorption/ionization time of flight (MALDI-TOF) mass spectrum of 2-(2-pyridylmethyl)-1,3-dioxoisoindoline-5-carboxylic acid (HInMe-2-py).

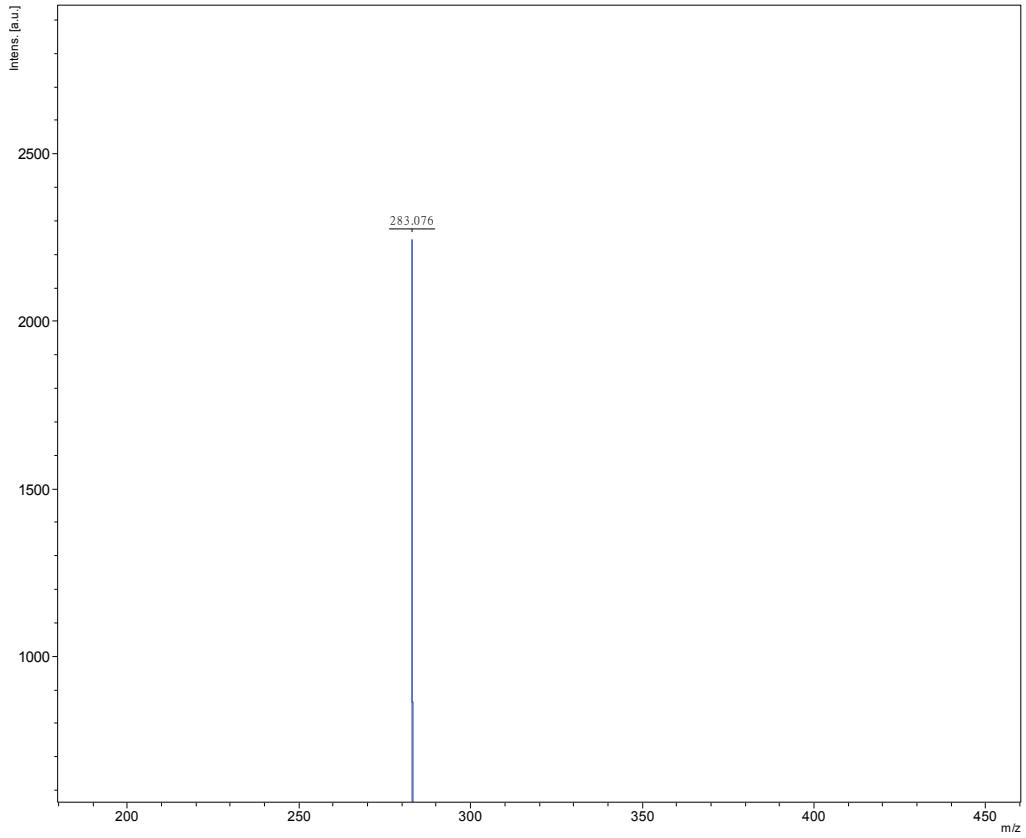

Fig. S5 Matrix-assisted laser desorption/ionization time of flight (MALDI-TOF) mass spectrum of 2-(3-pyridylmethyl)-1,3-dioxoisoindoline-5-carboxylic acid (HInMe-3-py).

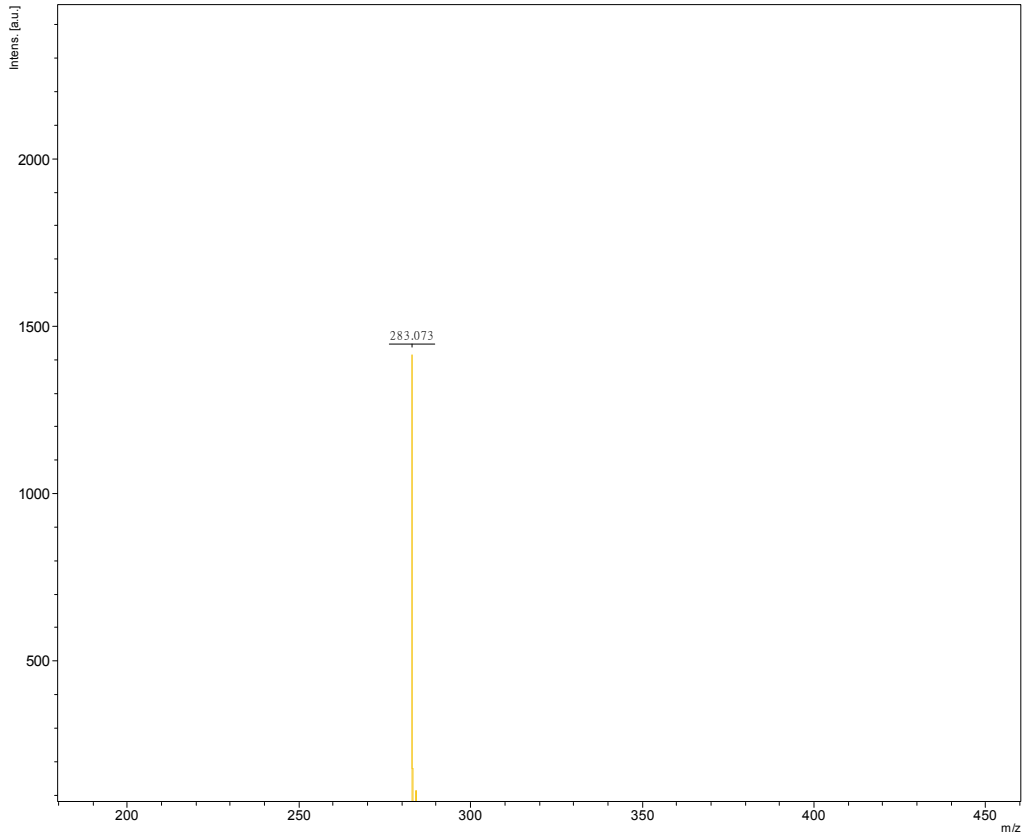

Fig. S6 Matrix-assisted laser desorption/ionization time of flight (MALDI-TOF) mass spectrum of 2-(4-pyridylmethyl)-1,3-dioxoisoindoline-5-carboxylic acid (HInMe-4-py).

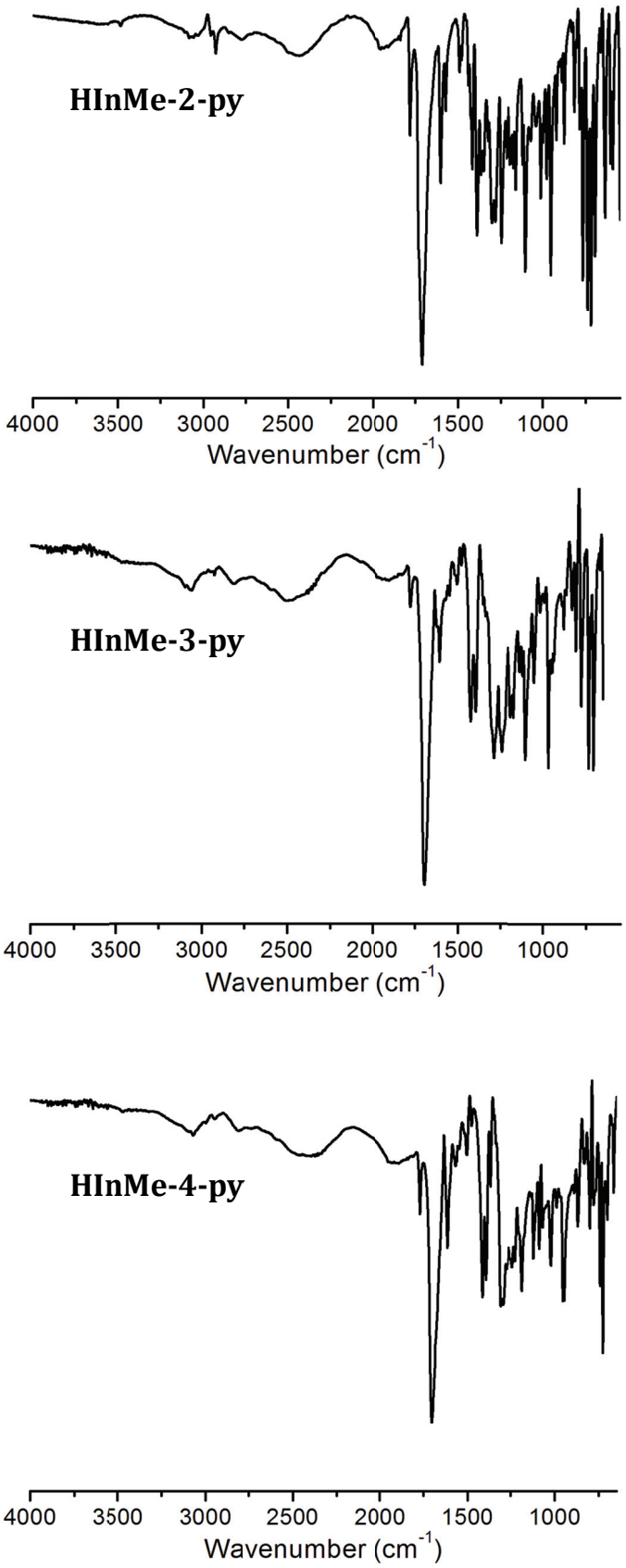

Fig. S7 Infrared (IR) spectra of HInMe-*n*-py (*n* = 2, 3, 4) ligands.

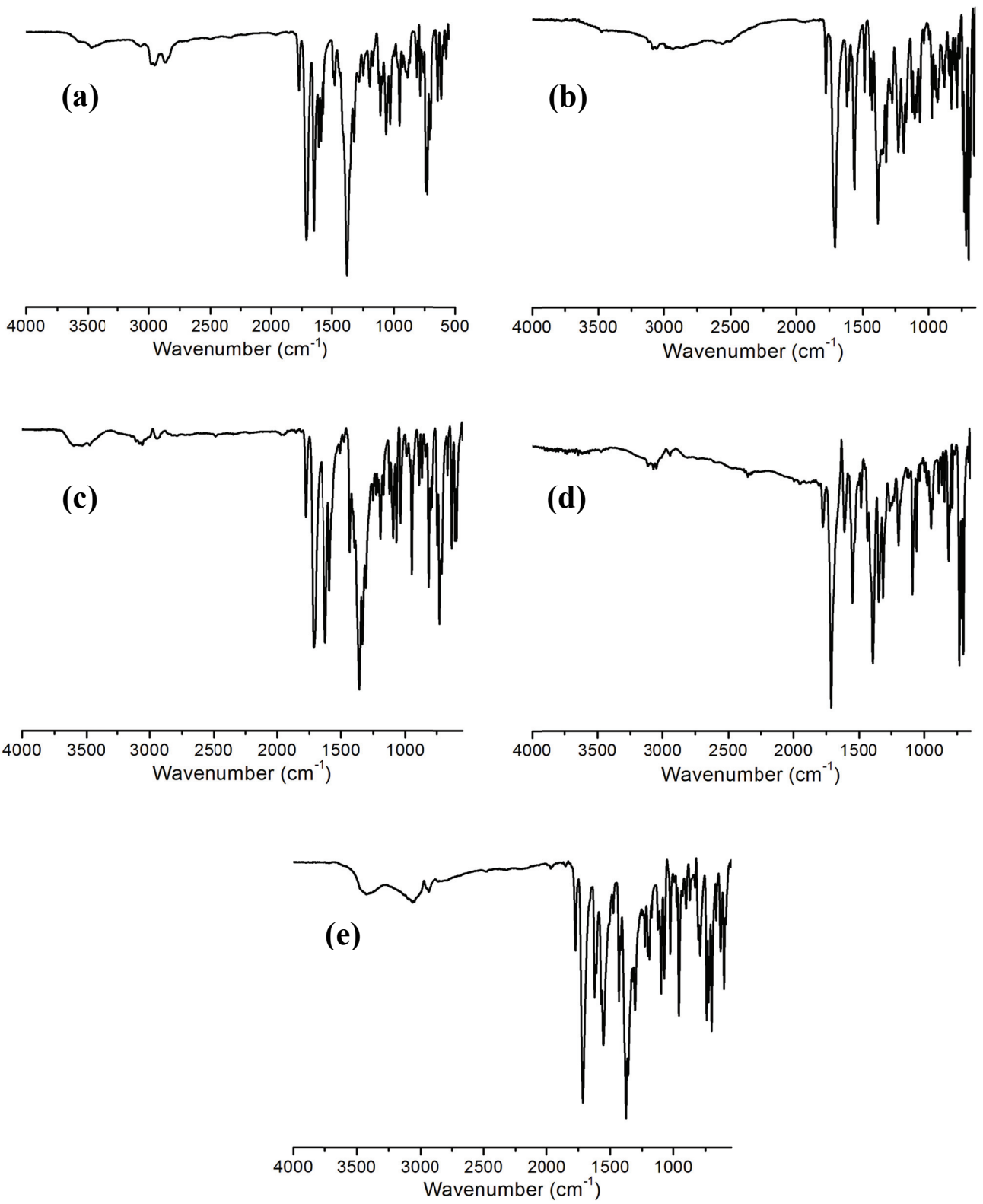

Fig. S8 Infrared (IR) spectra of (a–e) **1**–**5**.

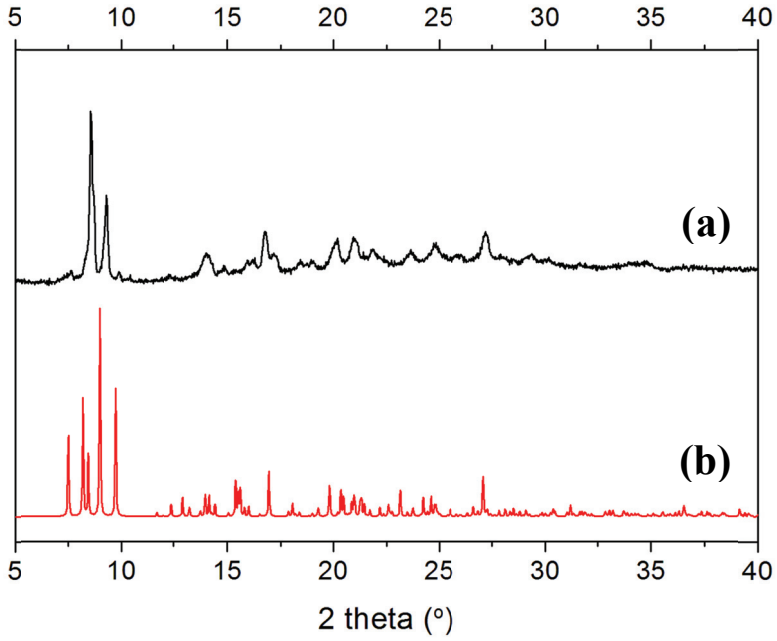

Fig. S9 X-Ray powder diffraction (XRPD) patterns of **1**: (a) a freshly grounded sample at room temperature; (b) simulated from the single-crystal data. For **1**, it is difficult to obtain a well-resolved XRPD pattern that is well-matched with the simulated XRPD patterns since lattice solvent molecules are gradually released during the XRPD measurement.

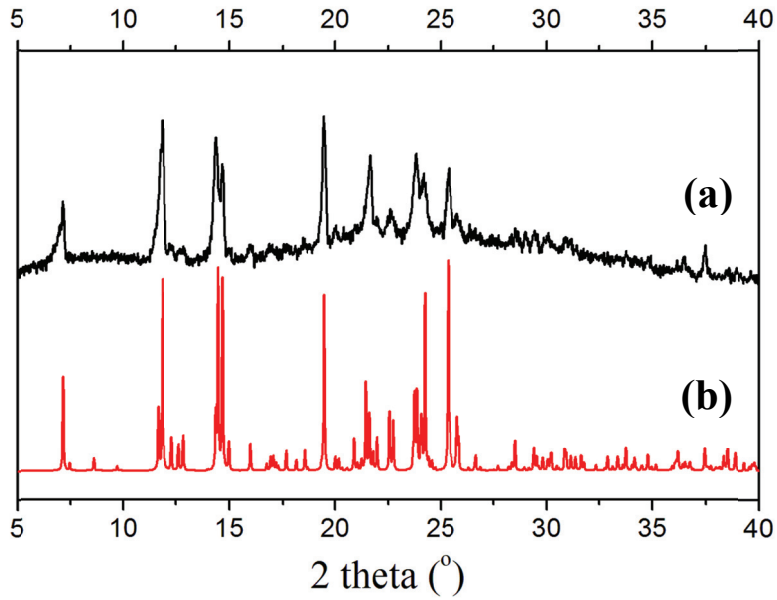

Fig. S10 X-ray powder diffraction (XRPD) patterns of **2**: (a) a freshly grounded sample at room temperature; (b) simulated from the single-crystal data.

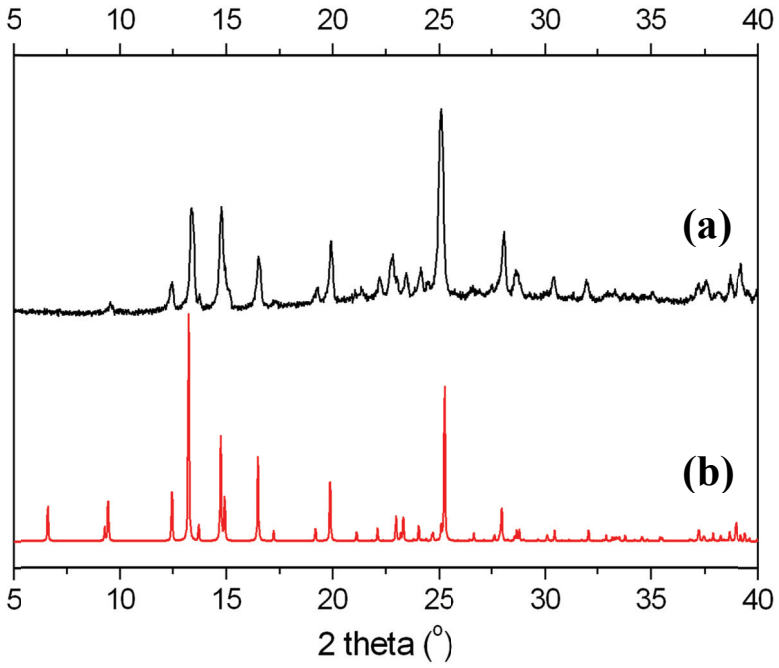

Fig. S11 X-Ray powder diffraction (XRPD) patterns of **3**: (a) a freshly grounded sample at room temperature; (b) simulated from the single-crystal data.

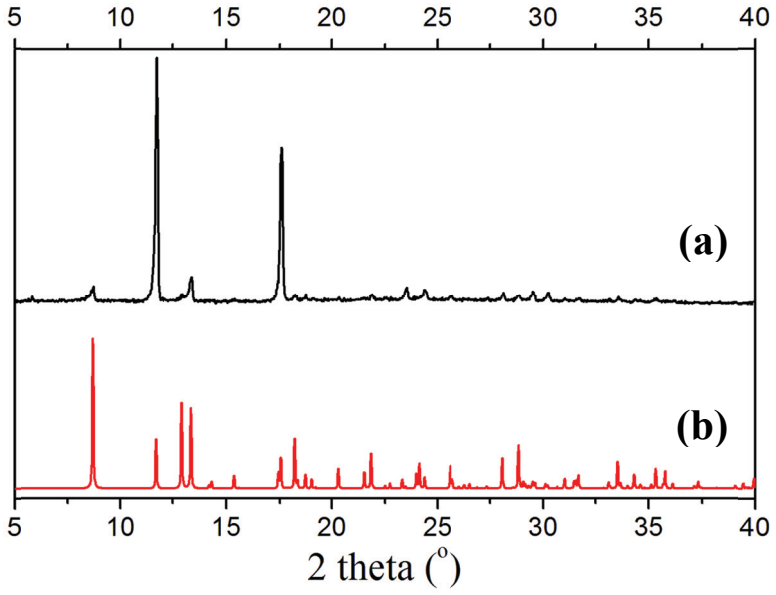

Fig. S12 X-Ray powder diffraction (XRPD) patterns of **4**: (a) a freshly grounded sample at room temperature; (b) simulated from the single-crystal data.

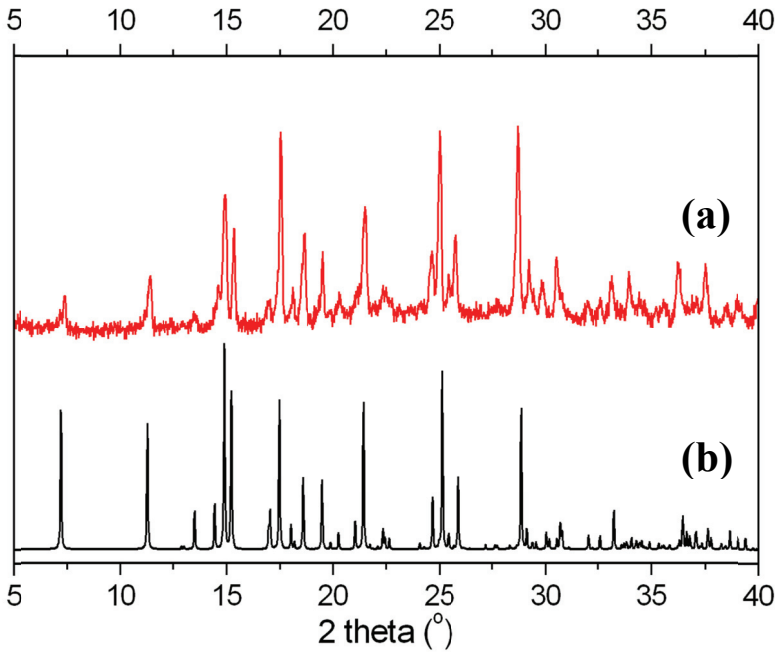

Fig. S13 X-Ray powder diffraction (XRPD) patterns of **5**: (a) a freshly grounded sample at room temperature; (b) simulated from the single-crystal data.

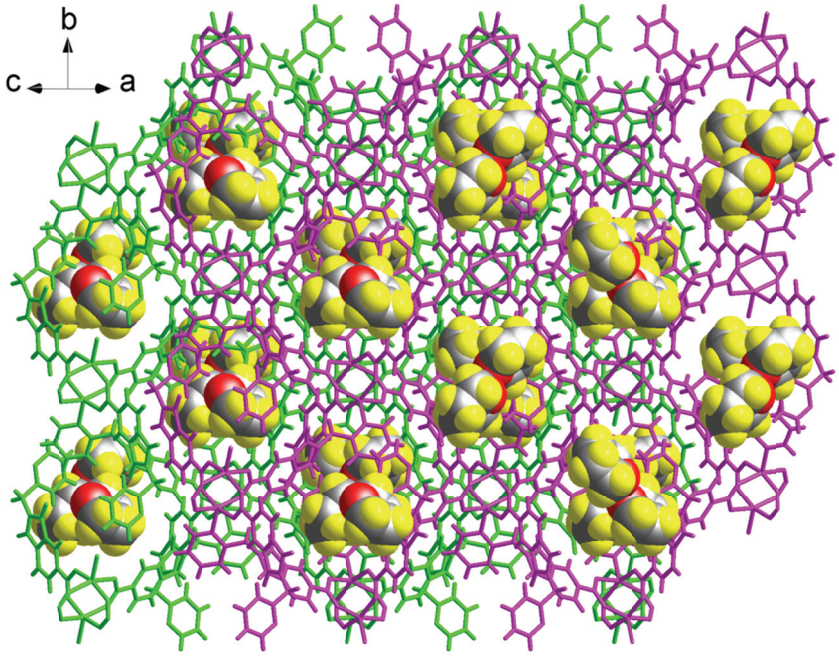

Fig. S14 Crystal packing of **1**, showing the lattice THF molecules (space-filling model) are accommodated within the cavities.

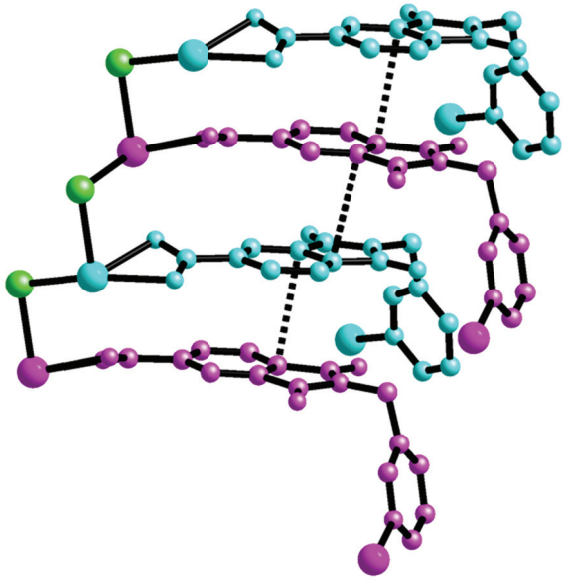

Fig. S15 Representation of the inter-helix π···π interactions (dashed lines, the shortest atom···atom distance: 3.3106(17) Å in **4**. Carbon-bound hydrogen atoms are omitted for clarity.

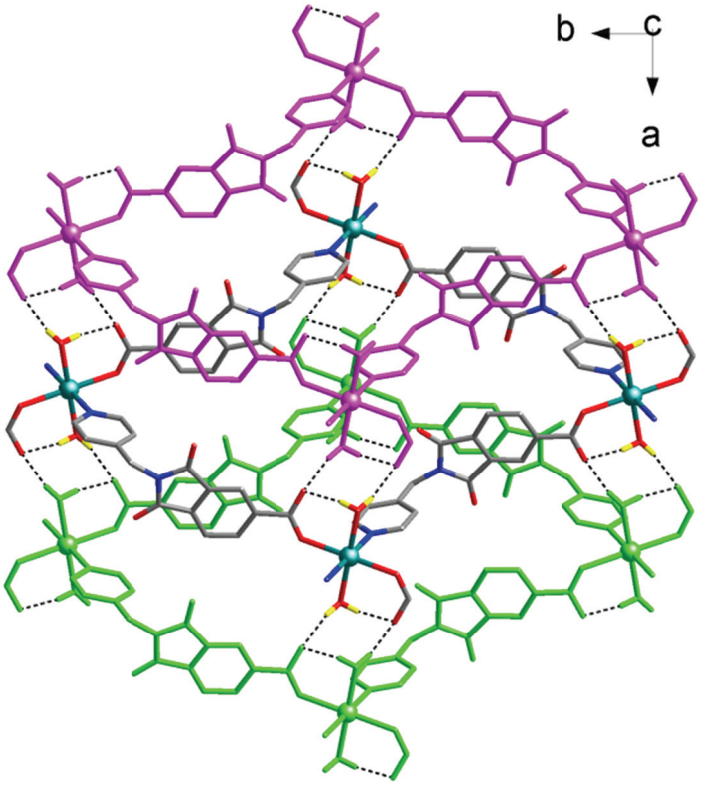

Fig. S16 Crystal packing of **5**, showing the three-dimensional hydrogen-bonded supramolecular net formed by net-to-net aqua–carboxylate hydrogen bonds (dashed lines). Carbon-bound hydrogen atoms are omitted for clarity.

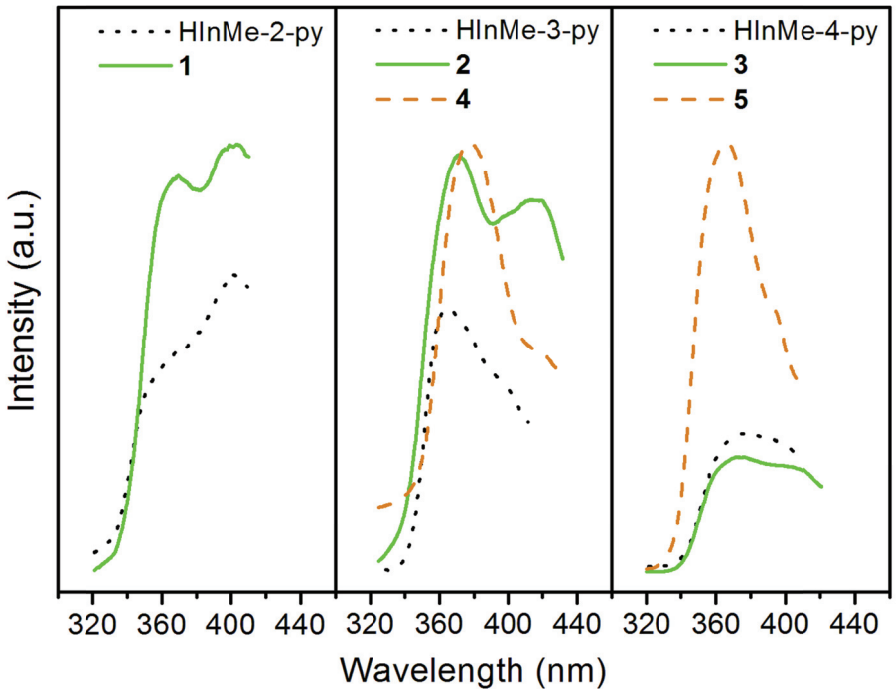

Fig. S17 Solid-state excitation spectra of HInMe-*n*-py (*n* = 2, 3, 4) ligands and compounds **1**–**5** at room temperature. *Note:* λ_{em} = 450 nm for HInMe-*n*-py (*n* = 2, 3, 4) ligands and **1**, λ_{em} = 470 nm for **2** and **4**, λ_{em} = 460 nm for **3**, and λ_{em} = 425 nm for **5**.